B7-H1–expressing antigen-presenting cells mediate polarization of protumorigenic Th22 subsets

Dong-Ming Kuang,[1,2] Xiao Xiao,[1] Qiyi Zhao,[1,3] Min-Min Chen,[1] Xue-Feng Li,[1] Rui-Xian Liu,[1] Yuan Wei,[1] Fang-Zhu Ouyang,[1] Dong-Ping Chen,[1] Yan Wu,[1] Xiang-Ming Lao,[2] Hong Deng,[3] and Limin Zheng[1,2]

[1]Key Laboratory of Gene Engineering of the Ministry of Education, State Key Laboratory of Biocontrol, School of Life Sciences, Sun Yat-sen University, Guangzhou, China. [2]State Key Laboratory of Oncology in Southern China, Cancer Center, Sun Yat-sen University, Guangzhou, China. [3]Department of Infectious Diseases, Third Affiliated Hospital, Sun Yat-sen University, Guangzhou, China.

Classical IL-22–producing T helper cells (Th22 cells) mediate inflammatory responses independently of IFN-γ and IL-17; however, nonclassical Th22 cells have been recently identified and coexpress IFN-γ and/or IL-17 along with IL-22. Little is known about how classical and nonclassical Th22 subsets in human diseases are regulated. Here, we used samples of human blood, normal and peritumoral liver, and hepatocellular carcinoma (HCC) to delineate the phenotype, distribution, generation, and functional relevance of various Th22 subsets. Three nonclassical Th22 subsets constituted the majority of all Th22 cells in human liver and HCC tissues, although the classical Th22 subset was predominant in blood. Monocytes activated by TLR2 and TLR4 agonists served as the antigen-presenting cells (APCs) that most efficiently triggered the expansion of nonclassical Th22 subsets from memory T cells and classical Th22 subsets from naive T cells. Moreover, B7-H1–expressing monocytes skewed Th22 polarization away from IFN-γ and toward IL-17 through interaction with programmed death 1 (PD-1), an effect that can create favorable conditions for in vivo aggressive cancer growth and angiogenesis. Our results provide insight into the selective modulation of Th22 subsets and suggest that strategies to influence functional activities of inflammatory cells may benefit anticancer therapy.

Introduction

IL-22 is a member of the IL-10 family that induces the production of chemokines and antimicrobial peptides by cells in tissues (1–3). Besides possible involvement in host defense against microbes, this cytokine has been linked to the pathogenesis of several inflammatory and autoimmune diseases (4–6). In animal models, it has been shown that IL-22 plays an important role in regulating autoimmune encephalitis, collagen-induced arthritis, colitis, and psoriasis (2, 7, 8). In humans, increased levels of IL-22–producing cells have been observed in epidermis from individuals with inflammatory skin disorders, and the IL-22$^+$ T cell clone derived from psoriasis patients can enhance wound healing and tissue remodeling, an effect that depends exclusively on IL-22 (2, 9).

Although IL-22 was originally assumed to be a T helper type 1–associated (Th1-associated) cytokine (1, 2, 10), it has subsequently been linked to expression of IL-17 in Th17 cells (11–13). More recently, a novel IL-22–producing Th cell subset designated classical Th22 was described in humans and found to be unrelated to IFN-γ and IL-17 (14, 15). Nevertheless, it has been emphasized that a considerable proportion of IL-22$^+$ Th cells from inflamed human tissues can coproduce IFN-γ and/or IL-17, and these can be called nonclassical Th22 cells (9). Thus, data on the composition and immune function of Th22 subsets in local environments are essential for understanding the potential mechanisms of these cells in immunopathogenesis.

The precise mechanisms of Th22 polarization are not yet clear, and this applies in particular to the nonclassical Th22 subsets in humans. A related issue that must be addressed is the nature of the antigen-presenting cells (APCs) that are capable of inducing Th22 responses. Here, we found that nonclassical Th22 cells represented about 80% of the entire Th22 population in tissues of normal human liver and tumor. Monocytes activated by LPS were the APCs that most efficiently triggered the expansion of nonclassical Th22 cells from memory T cells and classical Th22 cells from naive T cells. Selective repression of IFN-γ–producing Th22 subsets occurred in hepatocellular carcinoma (HCC) tissue, and blockade of B7-H1 on tumor monocytes directed Th22 cell differentiation away from IL-17 and toward IFN-γ. Moreover, we found evidence that an increase in IL-17–expressing Th22 cells in HCC promoted aggressive cancer growth and angiogenesis.

Results

Th22 subset composition in human blood and tissue. We used FACS to analyze the composition of IL-22–producing Th subsets in 12 normal blood samples, 4 normal liver samples (tissue distal to a liver hemangioma), and 26 HCC tumor samples paired with peritumoral liver and blood samples (Supplemental Table 1; supplemental material available online with this article; doi:10.1172/JCI74381DS1). We classified 8 Th22 subsets based on their abilities to secrete IFN-γ, IL-4, and/or IL-17 (Figure 1A). In all the samples we analyzed, the four IL-4–producing Th22 subsets represented only a very small proportion (0.05% to ~2.7%), whereas 4 other subsets, including the classical Th22 (IFN-γ$^-$IL-17$^-$), Th22/Th1 (IFN-γ$^+$IL-17$^-$), Th22/Th17 (IFN-γ$^-$IL-17$^+$), and Th22/Th17/

Conflict of interest: The authors have declared that no conflict of interest exists.
Submitted: November 20, 2013; **Accepted:** August 8, 2014.
Reference information: *J Clin Invest*. 2014;124(10):4657–4667. doi:10.1172/JCI74381.

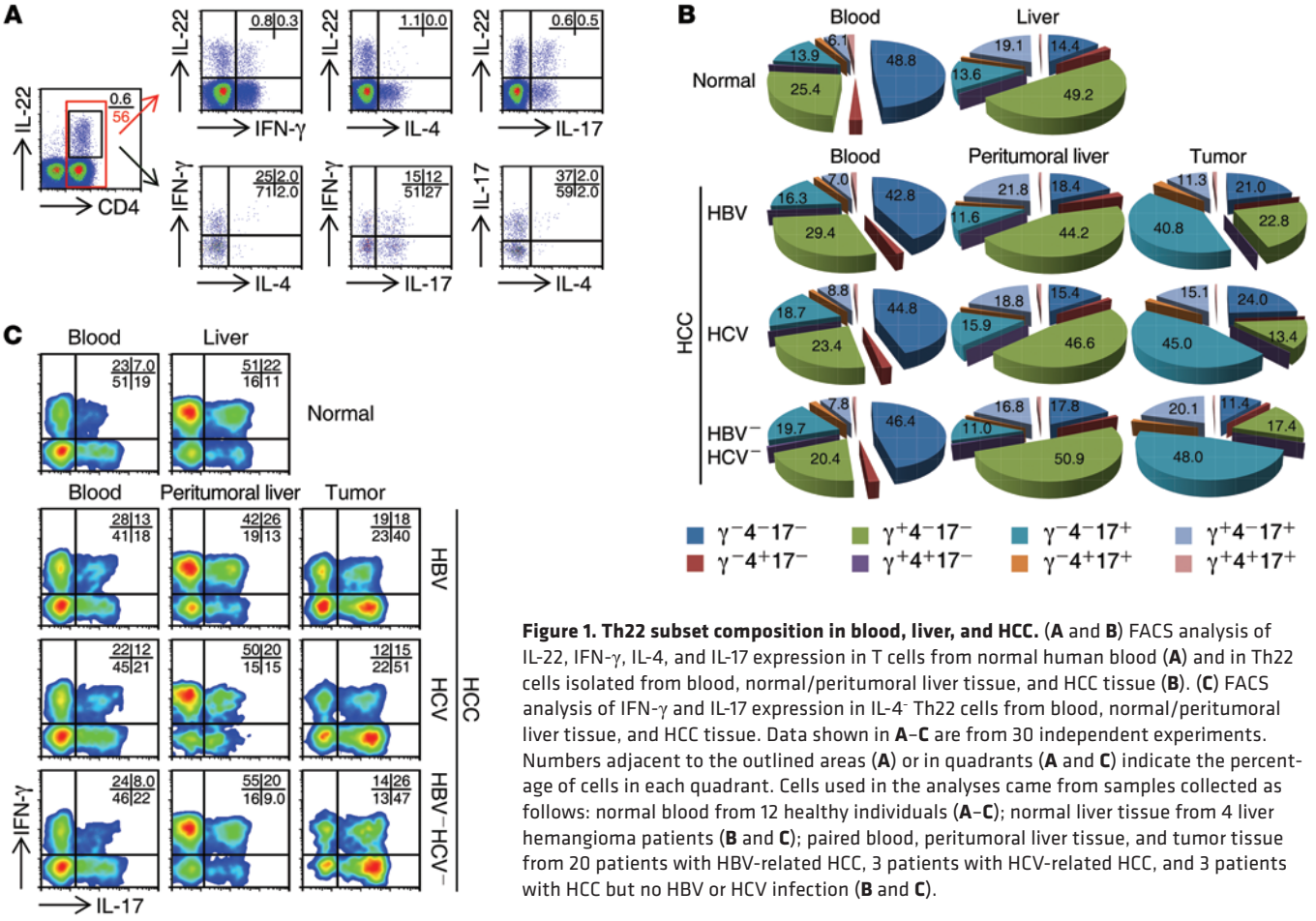

Figure 1. Th22 subset composition in blood, liver, and HCC. (**A** and **B**) FACS analysis of IL-22, IFN-γ, IL-4, and IL-17 expression in T cells from normal human blood (**A**) and in Th22 cells isolated from blood, normal/peritumoral liver tissue, and HCC tissue (**B**). (**C**) FACS analysis of IFN-γ and IL-17 expression in IL-4⁻ Th22 cells from blood, normal/peritumoral liver tissue, and HCC tissue. Data shown in **A**–**C** are from 30 independent experiments. Numbers adjacent to the outlined areas (**A**) or in quadrants (**A** and **C**) indicate the percentage of cells in each quadrant. Cells used in the analyses came from samples collected as follows: normal blood from 12 healthy individuals (**A**–**C**); normal liver tissue from 4 liver hemangioma patients (**B** and **C**); paired blood, peritumoral liver tissue, and tumor tissue from 20 patients with HBV-related HCC, 3 patients with HCV-related HCC, and 3 patients with HCC but no HBV or HCV infection (**B** and **C**).

Th1 (IFN-γ⁺IL-17⁺) cells, constituted 96.5% ± 2.4% (Figure 1B). Classical Th22 cells constituted the predominant subset (~50% of total Th22 cells) in blood from both healthy donors (n = 12) and HCC patients (n = 26) (Figure 1, B and C). We found increased proportions of IFN-γ–associated Th22/Th1 and Th22/Th17/Th1 cells (44.2 ± 8.3% and 21.8 ± 4.7%, respectively) in both normal and peritumoral liver tissues. However, compared with the peritumoral liver tissue, the tumor tissue contained a significant proportion of Th22/Th17 cells (40.8 ± 6.9%; n = 26, P < 0.001 compared with peritumoral liver Th22/Th17) accompanied by an attenuated amount of Th22/Th1 cells (22.8 ± 4.8%) (Figure 1, B and C). Also, the HCC patients who were infected with HBV or HCV and those without such infection exhibited a similar Th22 subset composition in blood and peritumoral liver and tumor tissues (Figure 1, B and C).

Phenotypic characteristics and transcription factor profiles of human Th22 subsets. Inasmuch as the classical Th22, Th22/Th1, Th22/Th17, and Th22/Th17/Th1 subsets constituted nearly the entire Th22 cell population, we next used FACS (Supplemental Figure 1) to investigate the phenotypic and transcriptional features of these subsets isolated from paired blood, peritumoral liver tissue, and HCC tumor tissue (Supplemental Table 1).

All the Th22 subsets, together with subsets Th1, Th17, and Th1/Th17, had a CD45RO⁺CD62L⁻CCR7⁻ effector memory phenotype exhibiting substantial expression of CCR4 and CCR6, but low or negligible expression of other chemokine receptors (Figure 2). A remarkably large portion of all the Th22 subsets expressed the proinflammatory cytokines IL-2 and TNF-α, but not the antiinflammatory IL-4, IL-9, and IL-10, which illustrates the proinflammatory properties of IL-22⁺ cells (Figure 2). Analysis of immune modulatory molecules on these subsets isolated from HCC tumor tissue revealed that both Th22/Th17/Th1 and Th22/Th17 cell subsets expressed higher levels of the activation markers HLA-DR, CD25, and CD69, as well as the regulatory molecules CTLA-4 and GITR, than did their subset counterparts Th1/Th17 and Th17, respectively (Figure 2, right panel). These results suggest that IL-22–related Th17 cells represent highly activated T cell subsets that express more inhibitory molecules to attenuate T cell responses in tumors. In contrast, the classical Th22, Th1, and Th22/Th1 subsets displayed only weak expression of the above-mentioned molecules (Figure 2).

We subsequently analyzed the transcription factors involved in the development of nonclassical Th22 subsets. The Th22/Th1 and Th22/Th17/Th1 subsets expressed T-bet at a high level, comparable to that exhibited by the Th1 and Th17/Th1 subsets; in parallel, RORγt was widely expressed by Th17 subsets. Consistently, the classical Th22 subsets expressed neither T-bet nor RORγt in any parts. We found that none of the analyzed Th cell subsets expressed the Treg-specific transcription factor FOXP3 (Figure 2). These results indicate that induction of IL-22 in human Th cells may be regulated by an unknown transcription factor different from that regulating Th1, Th17, and Tregs.

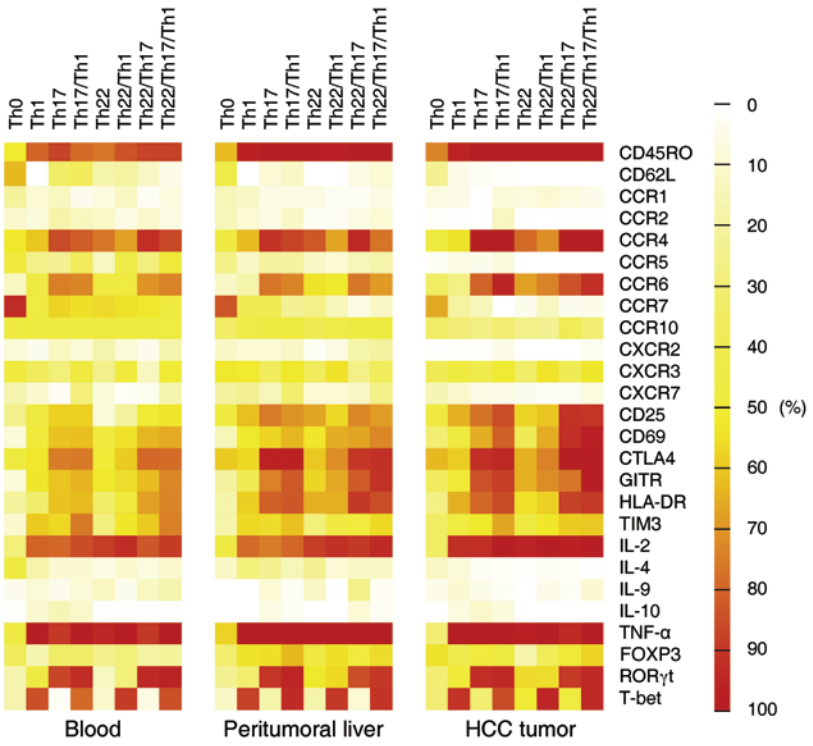

Figure 2. Phenotypic characteristics and transcription factor profiles of Th22 subsets. FACS analysis was performed to determine the phenotypic characteristics of Th0 (IFN-γ$^-$IL-17$^-$IL-22$^-$), Th1 (IFN-γ$^+$IL-17$^-$IL-22$^-$), Th17 (IFN-γ$^-$IL-17$^+$IL-22$^-$), Th17/Th1 (IFN-γ$^+$IL-17$^+$IL-22$^-$), Th22 (IFN-γ$^-$IL-17$^-$IL-22$^+$), Th22/Th1 (IFN-γ$^+$IL-17$^-$IL-22$^+$), Th22/Th17 (IFN-γ$^-$IL-17$^+$IL-22$^+$), and Th22/Th17/Th1 (IFN-γ$^+$IL-17$^+$IL-22$^+$) subsets isolated from blood, peritumoral liver tissue, and tumor tissue of HCC patients. Data for each of the indicated markers represent at least 4 patients. Data shown are from 30 independent experiments.

Activated APCs induce Th22 subset expansion. APCs are essential for initiating and maintaining the responses of Th cells (16–18). Having established the Th22 subset composition in human blood, liver, and HCC, we performed experiments to elucidate the nature of the APCs and innate stimuli that trigger the expansion and differentiation of Th22 subsets. We used freshly isolated monocytes from normal blood as well as cultured monocyte–derived macrophages (Mφ) (19) and DCs (20). APC activation was induced only by Pam3CysSK4 (a TLR2 agonist) and LPS (a TLR4 agonist), that is, not by CpG-DNA ODN (CpG, a TLR9 agonist) or poly (I:C) (PIC, a TLR3 agonist), as assessed by determining the upregulation of CD80 and CD86 (data not shown). The cytokine production in response to Pam3CysSK4 and LPS depended on the type of APCs present. In particular, monocytes produced larger amounts of TNF-α, IL-1β, IL-6, IL-23, and TGF-β, and, notably, this was not associated with production of IL-12p70 (Figure 3A).

In subsequent experiments, autologous T cells were incubated with monocytes, monocyte-derived Mφ or DCs, or such cells stimulated with LPS, and this was done in the absence or presence of CD3–cross-linking Abs. We measured T cell proliferation and production of IL-17, IFN-γ, and IL-22 on day 8 after incubation with IL-2. In general, all APCs induced T cell proliferation, although unstimulated APCs were much less potent than LPS-stimulated APCs in this context (Supplemental Figure 2A). LPS-activated monocytes were the APCs that most efficiently triggered expansion of Th22 cells (Figure 3B). Notably, most of these monocyte-expanded Th22 subsets were nonclassical (i.e., Th22/Th1, Th22/Th17, and Th22/Th17/Th1) (Figure 3C). In support of the view that IL-12p70 maintains Th1 responses, activated DCs mainly expanded the Th22/Th1 cell subset. We further purified naive and memory T cells and then cultured those cells with LPS-stimulated monocytes. The activated monocytes effectively promoted the expansion of Th22 cells from memory CD4$^+$ T cells, and most of the expanded cells were positive for IFN-γ and/or IL-17 (Figure 3D). By comparison, monocyte-primed naive T cells gave rise to only a moderate amount of Th22 cells, but over 80% of them showed the classical Th22 phenotype, which suggests that nonclassical Th22 cells are expanded from memory T cells and that classical Th22 cells are polarized from naive T cells.

To probe the mechanisms involved in the induction of Th22 cells by APCs, particularly activated monocytes, we used neutralizing Abs that effectively abolished the individual roles of the above-mentioned cytokines in our monocyte-expanded Th22 cell systems. Expression of IL-22 in CD4$^+$ T cells was inhibited 30%–60% by blocking IL-1β, IL-6, IL-23, or TGF-β, but was not reduced by blocking TNF-α alone (Supplemental Figure 2B). Precisely, blocking IL-1β mainly decreased the proportions of the IFN-γ–expressing Th22 cells, but an anti–TGF-β Ab primarily reduced the proportions of IL-17–producing Th22 cells (Figure 3E). In agreement with this, recombinant IL-1β effectively increased the prevalence of IFN-γ$^+$ Th22, and TGF-β selectively induced expansion of IL-17$^+$ Th22 cells (Supplemental Figure 2C). In addition, STAT proteins are well known for their essential roles in specifying Th cell differentiation. We found that conditioned media from APCs stimulated by LPS or Pam3CysSK4 could elicit marked activation of both STAT1 and STAT3, but not STAT5 or STAT6, in T cells in a time-dependent manner (Figure 3, F and G). Abolishing STAT1 activation by fludarabine effectively suppressed the LPS-activated mononcyte-mediated IFN-γ$^+$ Th22 expansion; in parallel, AG490, a specific inhibitor of STAT3, could effectively impair the generation of IL-17–related Th22 cells (Figure 3H).

Monocyte B7-H1 regulates the balance between IFN-γ$^+$ and IL-17$^+$ Th22 cells. After finding that Th22/Th17 cells selectively accumulated in HCC tissue, we evaluated the influence of HCC-infiltrating monocytes on the development of Th22 subsets. Compared with corresponding cells in blood, monocytes isolated from both peritumoral liver and tumor tissues expressed at least 10-fold higher levels of *TNFA*, *IL1B*, *IL6*, and *TGFB*, but not *IL12A* (Figure 4A). Furthermore, analysis of immune modulatory molecules on monocytes revealed that only such cells isolated from tumor tissue showed markedly elevated expression of coinhibitory B7-H1, although monocytes from both peritumoral liver and tumor tissues exhibited a CD80^{hi}CD86^{hi}HLA-DR^{hi}B7-H4$^-$ phenotype (Figure 4B), suggesting that B7-H1 regulates Th22/Th17 cells in tumors. To address this, we purified monocytes from peritumoral liver and

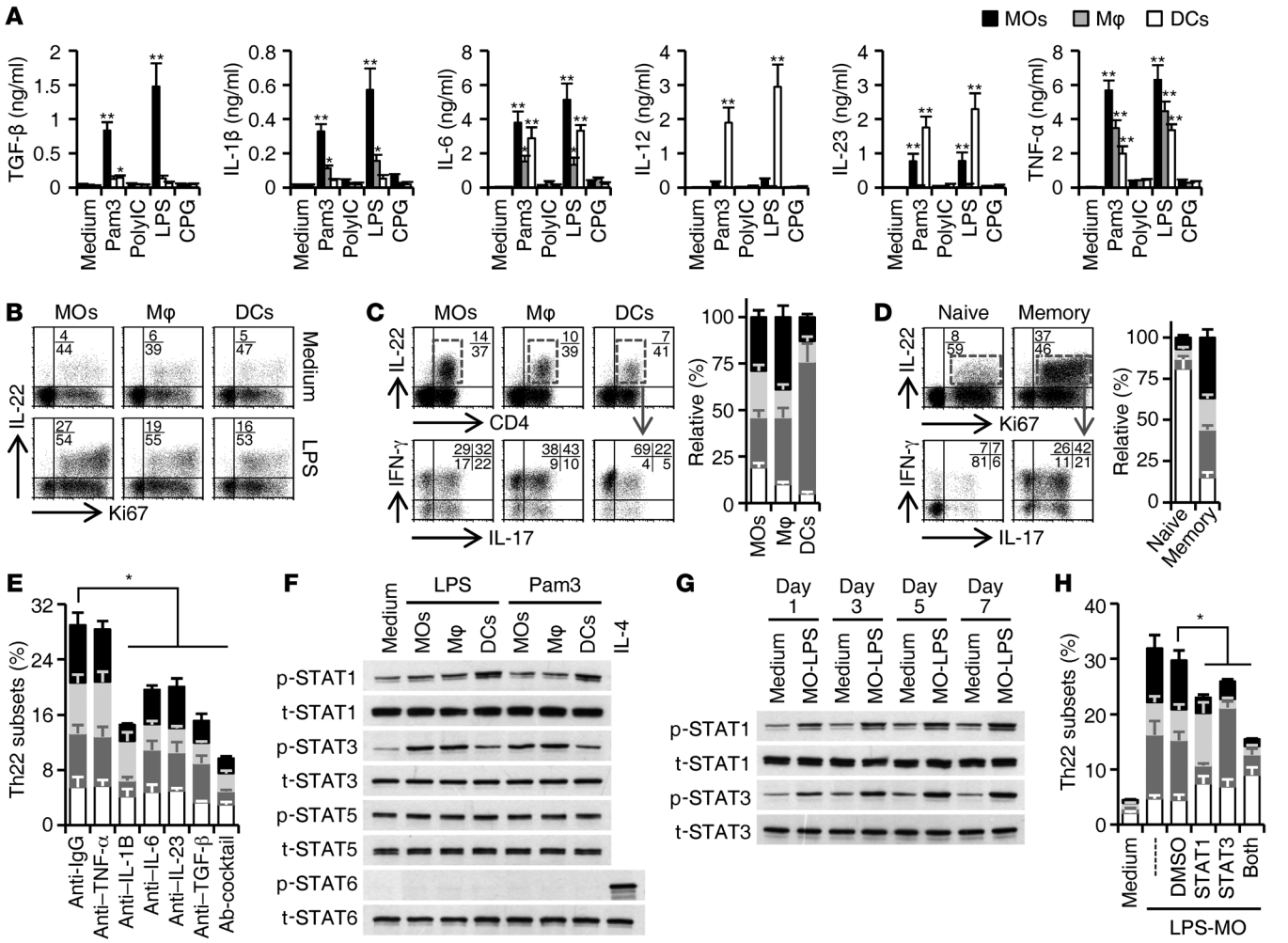

Figure 3. Activated APCs induce Th22 subset expansion. (**A**) Monocytes (MOs), Mφ, and DCs were left untreated or stimulated with Pam3CysSK4, LPS, poly (I:C), or CpG oligodeoxynucleotides (ODNs) for 18 hours. Cytokine production was determined by ELISA. (**B**–**D**) Monocytes, Mφ, or DCs were left untreated or stimulated with LPS for 5 hours and then cultured for 8 days with autologous T cells, naive T cells, or memory T cells as described in Methods. Proliferation (Ki67) and expression of IFN-γ and IL-17 in Th22 cells were detected by FACS. Numbers in quadrants indicate the percentage of cells in each quadrant. (**E**) Blockade of TNF-α, IL-1β, IL-6, IL-23, and/or TGF-β changed the subset composition of Th22 cells expanded by LPS-stimulated monocytes. (**F** and **G**) T cells were left untreated or cultured with conditioned media from LPS- or Pam3CysSK4-stimulated monocytes, Mφ, or DCs for 7 days (**F**) or for the indicated times (**G**), as described in Methods. Activation of STAT proteins was detected by immunoblotting. IL-4–treated T cells served as a positive control. (**H**) Inhibiting STAT1 and STAT3 activation changed the subset composition of Th22 cells expanded by LPS-stimulated monocytes. Th22 subset composition was determined by FACS. Th22 subset composition is shown in **C**–**E** and **H**: classical Th22, white bar; Th22/Th1, dark gray bar; Th22/Th17, light gray bar; Th22/Th17/Th1, black bar. Data represent the mean ± SEM (**A**, **C**–**E**, and **H**). Results in all panels represent 5 separate experiments (n = 5–7). $^*P < 0.05$ and $^{**}P < 0.01$, compared with untreated cells (**A**) or the indicated groups.

paired tumor tissues and then cultured those cells together with autologous peripheral T cells. The monocytes from both sources markedly expanded Th22 cells, albeit with a subset bias: the peritumoral monocytes promoted expansion of IFN-γ–producing Th22 cells more strongly, whereas tumor monocytes associated selectively with the IL-17–expressing Th22 cell subset (Figure 4C). In support of our hypothesis, blocking B7-H1 by preincubating tumor monocytes with the mAb MIH1 led to a marked increase in Th22 cells that were related to IFN-γ (Figure 4C). Notably, such treatment also elicited robust production of IL-22 and IFN-γ by T cells (Supplemental Figure 3).

Considering that B7-H1 was also expressed by the LPS-activated monocytes (Supplemental Figure 4A), we subsequently analyzed the involvement of this protein in LPS-stimulated monocyte-mediated Th22 subset bias. We found that blocking B7-H1 markedly and consistently increased the proportion of IFN-γ–producing Th22 cells expanded by exposure to LPS-activated monocytes (Figure 4D). Furthermore, we transduced HEK293T cells with pBABE-Puro retroviral vector encoding human B7-H1 or B7-DC (Supplemental Figure 4B) and then cultured those cells with T cells in a cytokine-expanded Th22 system. B7-H1–expressing HEK293T cells could effectively suppress the cytokine-mediated early STAT1 activation and IFN-γ production in T cells and later Th1-related Th22 polarization; the effects could be reversed by the B7-H1–blocking mAb MIH1 (Figure 4, E and F, and Supplemental Figure 5). These results suggest that the B7-H1/PD-1 inhibitory pathway negatively regulates STAT1 by limiting IFN-γ production, which in turn suppresses Th1-related subset develop-

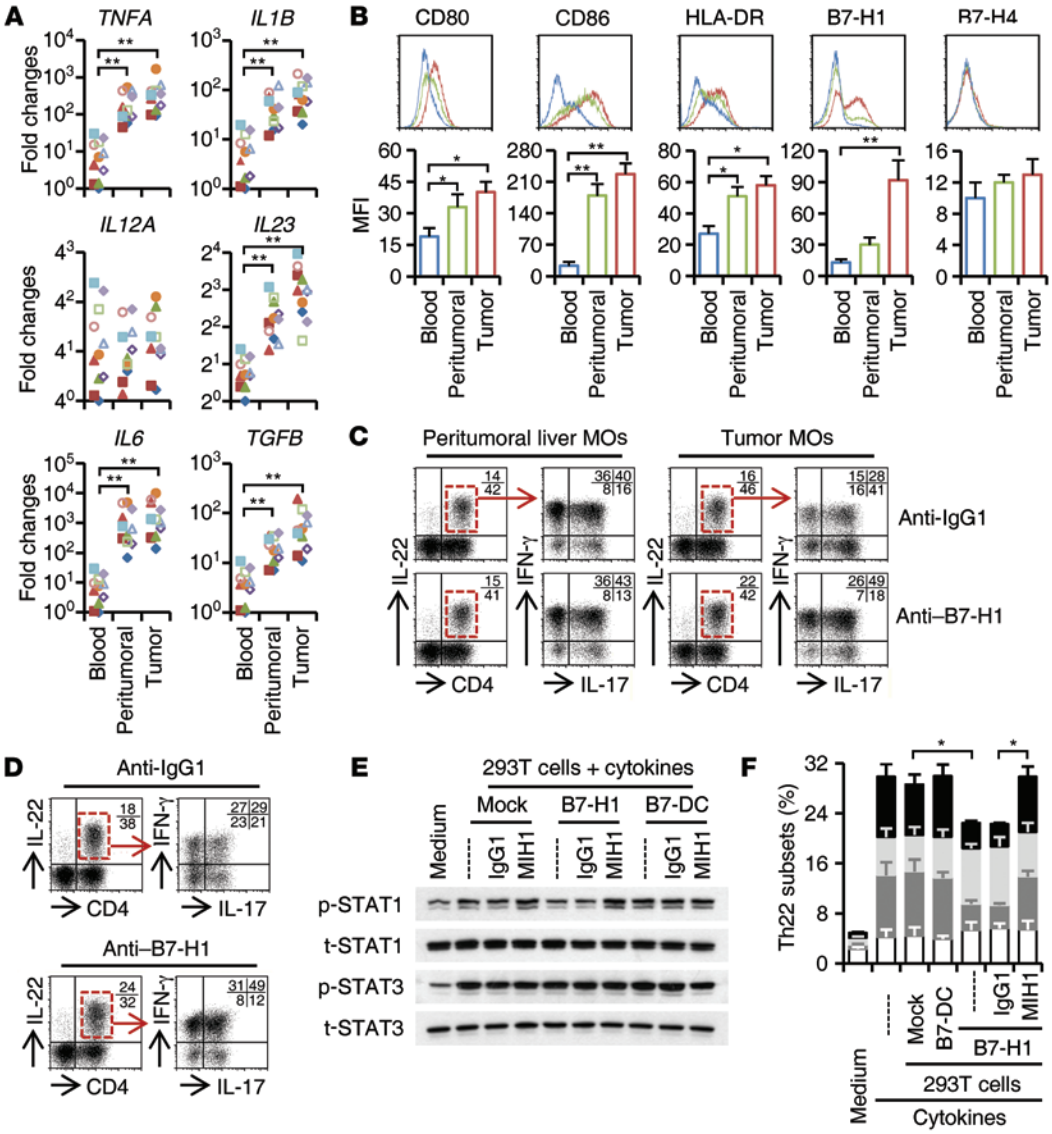

Figure 4. Monocyte B7-H1 regulates the balance between IFN-γ– and IL-17–related Th22 cells. (**A**) Real-time PCR determination of relative fold changes in the indicated cytokine mRNAs in monocytes from paired samples of blood and peritumoral liver and tumor tissues from 11 HCC patients. (**B**) FACS analysis of expression of the indicated markers on monocytes from paired samples of blood and peritumoral liver and tumor tissues from 4 HCC patients. (**C** and **D**) Purified T cells were cultured for 8 days with autologous peritumoral liver or tumor monocytes (**C**) or LPS-stimulated peripheral monocytes (**D**) in the presence of an anti–B7-H1 or a control Ab, as described in Methods. Expression of IL-22 in Th cells and expression of IFN-γ and IL-17 in Th22 are shown. Numbers in quadrants indicate the percentage of cells in each quadrant. (**E** and **F**) T cells were left untreated or were cultured with mock, B7-H1, or B7-DC transfectant in the presence of IL-1β, IL-6, IL-23, and TGF-β for 9 days as described in Methods. In parallel, B7-H1–expressing transfectants were preincubated for 1 hour with an anti–B7-H1 or a control Ab. STAT activation on day 1 (**E**) and Th22 subset composition on day 8 (**F**) in T cells were determined by immunoblotting and FACS, respectively. Th22 subset composition is shown in **F**: classical Th22, white bar; Th22/Th1, dark gray bar; Th22/Th17, light gray bar; Th22/Th17/Th1, black bar. Data represent the mean ± SEM (**B** and **F**). Results represent 4 separate experiments (n = 4–6; **C**–**F**). $^*P < 0.05$; $^{**}P < 0.01$.

ment. We found that the B7-DC transfectant did not affect such processes (Figure 4, E and F and Supplemental Figure 5).

Repression of IFN-γ–producing Th22 subsets in human HCC. IFN-γ–producing Th22 cells were repressed by the monocyte B7-H1 ex vivo, which prompted us to analyze the association between the proportions of Th22 and PD-1$^+$ Th cells in HCC. Upregulation of all Th22 subsets was much more pronounced in tumor and peritumoral liver tissues than in blood from HCC patients (n = 26) (Figure 5A). Due to declines in IFN-γ–related Th22 cell subsets, the prevalence of all Th22 cells was lower in the tumor samples than in the paired peritumoral liver samples, although we found significantly more IL-17–producing Th22 cells in tumor tissue than in peritumoral liver tissue (Figure 5B) (2.1 ± 0.3% and 0.7 ± 0.1% in CD4$^+$ T cells, respectively; n = 26 for both). Contrary to the infiltration pattern of the entire Th22 cell population, the proportion of PD-1$^+$ Th cells was markedly increased in tumor tissue (60 ± 13%, n = 26; $P < 0.001$ compared with proportions in blood and peritumoral liver tissue; Figure 5C). As expected, in the tissues, the proportions of PD-1$^+$ Th cells were inversely correlated with both the size of the entire Th22 cell population and the proportions of the IFN-γ–producing Th22 subsets (Figure 5, D and E), whereas the levels of PD-1$^+$ Th cells differed from the proportions of IL-17–

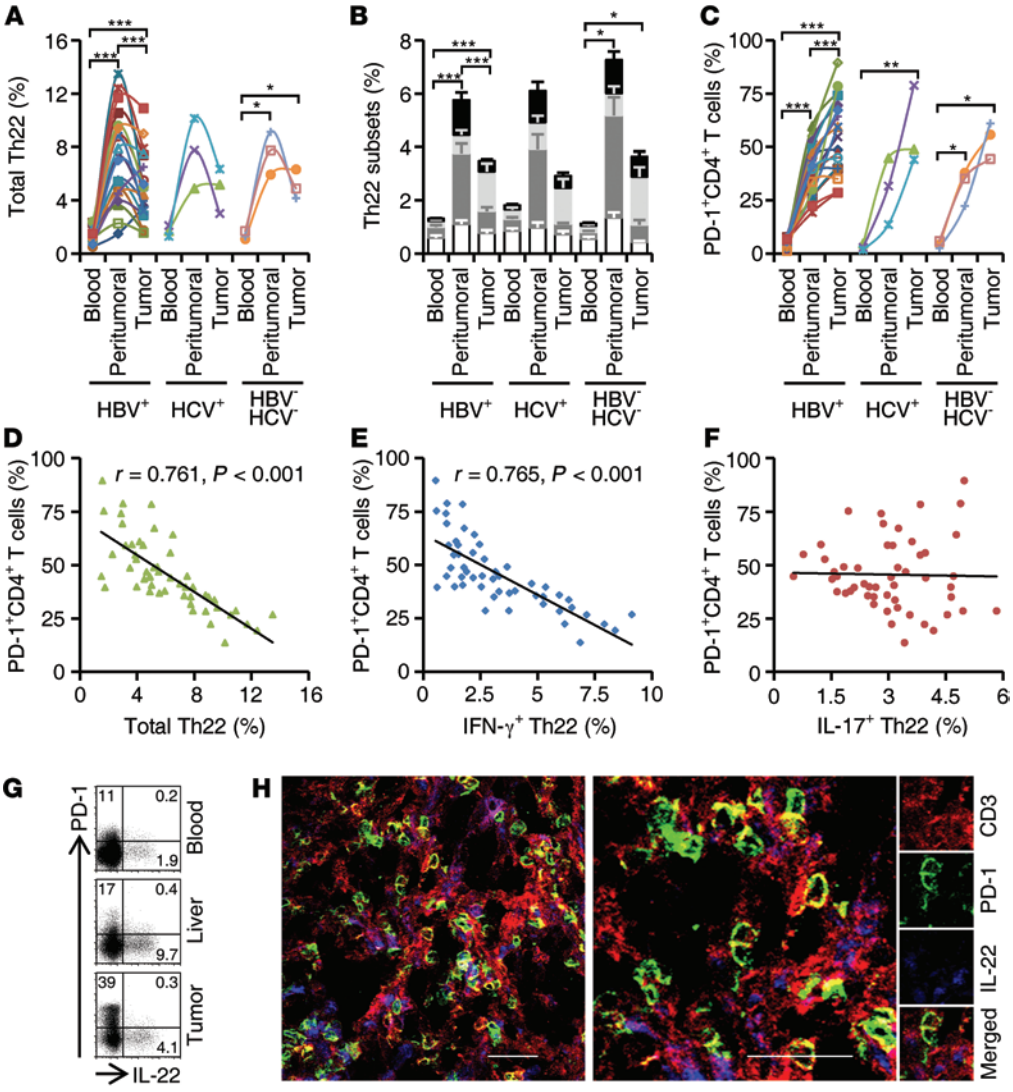

Figure 5. Repression of IFN-γ–producing Th22 subsets in human HCC. (**A**) FACS analysis of IL-22 expression in fresh Th cells isolated from paired blood and peritumoral liver and tumor tissues. (**B**) FACS analysis of Th22 subset composition in Th cells isolated from paired blood and peritumoral liver and tumor tissues: classical Th22, white bar; Th22/Th1, dark gray bar; Th22/Th17, light gray bar; Th22/Th17/Th1, black bar. Data represent the mean ± SEM. (**C**) FACS analysis of PD-1 expression on Th cells isolated from paired blood and peritumoral liver and tumor tissues. (**D**–**F**) Correlations between the levels of PD-1$^+$ Th cells and the following cells isolated from samples of peritumoral liver and tumor tissues from HCC patients (n = 26): total Th22 cells (**D**), IFN-γ$^+$ Th22 cells (**E**), and IL-17$^+$ Th22 cells (**F**). (**G**) Expression of IL-22 and PD-1 in Th cells isolated from paired samples of blood and peritumoral liver and tumor tissues from 8 HCC patients. Numbers in quadrants indicate the percentage of cells in each quadrant. (**H**) Expression of IL-22, PD-1, and CD3 in HCC tumor tissue. One of 5 representative micrographs is shown. Scale bars: 40 μm. Cells analyzed in **A**–**C** were isolated from samples collected from 20 patients with HBV-related HCC, 3 patients with HCV-related HCC, and 3 patients with HCC but no HBV or HCV infection. *P < 0.05; **P < 0.01; ***P < 0.001.

expressing Th22 cells (Figure 5F). We observed analogous changes in the proportions of Th22 and PD-1$^+$ Th cells in tissues that were or were not infected with hepatitis B virus (HBV) or hepatitis C virus (HCV) (Figure 5, A–C). Furthermore, both confocal microscopy and FACS confirmed that IL-22 protein was expressed mainly in PD-1$^-$ Th cells (n = 8) and only weakly in PD-1$^+$ cells (Figure 5, G and H).

Protumorigenic role of Th22 and Th17 in HCC. Previous studies have shown that IL-22 exhibits protumorigenic activity in several types of human cancers (21–26). To evaluate the potential role of IL-22 and its related subsets in HCC pathogenesis, we divided the 26 HCC patients described above into 2 groups according to their complete clinical and pathological characteristics. Figure 6A shows that the proportions of Th22 cells were associated with the patients' tumor node metastasis (TNM) stages and intrahepatic metastasis in the tumor samples but not in the peritumoral liver tissue, which implies an unfavorable effect on patient survival. We investigated this possibility by immunohistochemical staining of IL-22 in paraffin-embedded tissues from 197 HCC patients (Supplemental Table 2). Kaplan-Meier analysis showed inverse associations between IL-22$^+$ cell density in the tumor area and both overall survival (OS) (P < 0.001) and disease-free survival (DFS) (P < 0.0001) (Figure 6, B and C). In multivariate analysis, the number of IL-22$^+$ cells in the tumor region was an independent prognostic factor for both OS and DFS (Supplemental Table 3).

Th22 cells in peritumoral liver tissue produced higher levels of IFN-γ, whereas those in tumor tissue were selectively associated with IL-17 (Figure 5B). Therefore, we investigated the role of IL-22 alone or in combination with IFN-γ or IL-17 in regulating the biological behavior of hepatoma. We exposed hepatoma cells to IL-22 for 10 hours under serum starvation, which resulted in a markedly altered phenotype exhibiting active phosphorylation of the *STAT3* oncogene and pronounced upregulation of survival-associated Mcl-1 and cell cycle–related CDK4, C-Myc, and cyclin D1 (Figure 6D and Supplemental Figure 6). However, adding IFN-γ completely abolished such proproliferative and prosurvival roles of IL-22. Notably, IFN-γ also increased expression of proapoptotic BAX and BID in IL-22–treated hepatoma cells, whereas the addition of IL-17 had only a marginal effect on hepatoma cell survival and proliferation (Figure 6D and Supplemental Figure 6). Consistent with these in vitro findings, we observed that injection of T cells polarized by tumor monocytes in the presence of anti–B7-H1

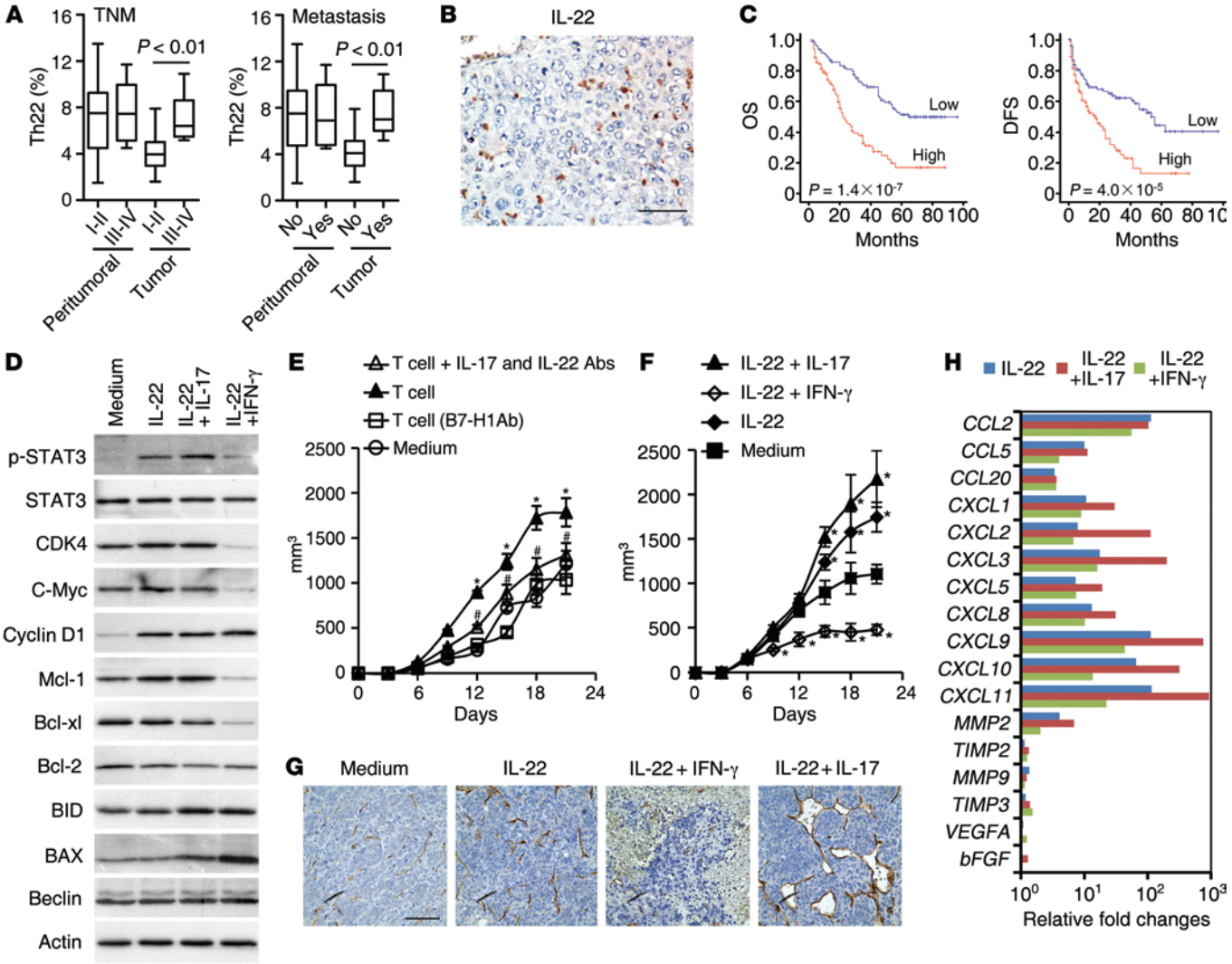

Figure 6. Protumorigenic roles of IL-22 and IL-17 in HCC. (**A**) Correlations between proportions of Th22 cells in tumor tissue from 26 patients and TNM or intrahepatic metastasis in patients. (**B** and **C**) Paraffin-embedded hepatoma samples were stained with an anti–IL-22 Ab. Scale bar: 50 μm. Based on the median value of IL-22$^+$ cell density, patients were divided into low-density (n = 99) and high-density (n = 98) groups; cumulative OS and DFS times were calculated by the Kaplan-Meier method and analyzed by a log-rank test (**C**). (**D** and **H**) IL-22 plus IL-17 promoted the survival, proliferation, and proangiogenic activities of hepatoma cells. HepG2 cells undergoing serum starvation were stimulated with IL-22 alone or combined with IL-17 or IFN-γ (50 ng/ml for all) for 10 hours. Expression of the indicated proteins and genes (given as the mean) was determined by immunoblotting and real-time PCR, respectively. Results are representative of 4 separate experiments (n = 4–6). (**E**) Injection of T cells polarized by tumor monocytes significantly enhanced HepG2 hepatoma growth in mice; the effects were attenuated by additional injection of neutralizing Abs against IL-22 and IL-17. Data represent the mean ± SEM of 5 independent experiments (n = 6 for each). *P < 0.05, compared with the Medium group; #P < 0.05, compared with the T cell group (without B7-H1 mAb). (**F** and **G**) IL-22 plus IL-17 promoted the growth and angiogenesis of hepatoma in mice. Data represent the mean ± SEM (n = 5 for each group). *P < 0.05. Paraffin-embedded hepatoma samples were stained with an anti-CD34 Ab (**G**). Scale bar: 100 μm.

mAb (25.1 ± 3.4% and 21.3 ± 2.9% of them were IFN-γ$^+$ Th22 cells and IL-17$^+$ Th22 cells, respectively; n = 6) only marginally affected the growth of human hepatoma. In contrast, the injection of T cells polarized by tumor monocytes without anti–B7-H1 mAb (10.5 ± 2.7% and 23.2 ± 3.2% of them were IFN-γ$^+$ Th22 cells and IL-17$^+$ Th22 cells, respectively) significantly enhanced the tumor growth (Figure 6E). Supporting our hypothesis that IL-22 and IL-17 signals contribute to disease progression, administration of anti–IL-22– and anti–IL-17–neutralizing Abs effectively suppressed the protumorigenic effect of T cells polarized in the absence of B7-H1 mAb (Figure 6E). Similar results were obtained in another in vivo system, showing that the protumorigenic effect of IL-22 was completely reversed by adding IFN-γ, but was accelerated by IL-17 supplement (Figure 6F). Data from immunohistochemical staining revealed that IL-17 additionally increased IL-22–mediated angiogenesis (Figure 6G).

We further investigated the potential role of IL-22 in angiogenesis using real-time PCR analysis. Compared with untreated hepatoma cells, those exposed to IL-22 exhibited distinct upregulation of a set of proangiogenic genes including *CCL2*, *CCL5*, *CCL20*, *CXCL1*, *CXCL2*, *CXCL3*, *CXCL5*, *CXCL8*, *CXCL9*, *CXCL10*, *CXCL11*, and *MMP2*, and this process was enhanced by the addition of IL-17 but not IFN-γ (Figure 6H and Supplemental Figure 7). In support of this, we also found a significant correlation between

microvessel density (MVD) and the level of Th22 cells in human HCC tissue ($r = 0.728$, $P < 0.001$), whereas no such association was observed in peritumoral liver tissue ($r = 0.293$) (Supplemental Figure 8). Together, these results demonstrate that, in HCC, IL-22 plays a protumorigenic role that is potentiated by IL-17 in tumor tissue but counteracted by IFN-γ in peritumoral liver tissue.

Discussion

Despite recent success in demonstrating the existence of Th22 cells, little is known about the mechanisms underlying the regulation of different Th22 subsets in humans (8). The current study delineated the phenotype, distribution, generation, and functional relevance of various Th22 subsets in blood, liver, and HCC tissue.

Studies have identified a subset of epithelial Th effector cells that produce IL-22 (and are thus designated Th22) (9, 21), and it has been suggested that these cells participate in adaptive immunity and reorganization of epithelia via IL-22–mediated induction of antimicrobial peptides and genes involved in keratinocyte differentiation (27). In our investigation, the substantial proportion of Th22 cells in peritumoral liver and tumor tissues from HCC patients also secreted IFN-γ and/or IL-17, and reports have described such plasticity in other T cell phenotypes as well: for example, Th17 cells expressing IFN-γ and Tregs expressing IL-17 (28–31). Interestingly, we found that IFN-γ–expressing Th22 subsets were enriched predominantly in peritumoral liver tissue, and IL-17–producing Th22 subsets were selectively accumulated in HCC tissue. Further investigations revealed that the proportion of IL-17–producing Th22 cells in tumors correlated with aggressive angiogenesis, and the IL-17 cytokine could effectively enhance the proangiogenic effect of IL-22 both in vitro and in vivo. These findings imply that Th22 cells in tumor tissue, particularly those producing IL-17, do not represent the host defense against the malignancy, but instead reflect effects that are rerouted in a tumor-promoting direction by fostering angiogenesis. This notion is supported by our observations that the occurrence of Th22 cells in HCC tumor tissue, but not in peritumoral liver tissue, was positively associated with intrahepatic metastasis and TNM stages and also predicted shorter survival of the patients.

It is fairly well established that effector T cells are extremely heterogeneous in terms of cytokine production. We found that, along with classical Th22 subsets, nonclassical Th22 subsets constituted a major part of the IL-22–producing Th cells in tumor and peritumoral tissues from human liver, and most of these cells were expanded from memory T cells and spontaneously acquired the ability to produce IL-17 and IFN-γ. This finding agrees with studies suggesting that even though polarized T cells retain memory of the "imprinted" cytokine, they undergo further differentiation in response to polarizing cues (18, 32, 33). Alternatively, it is possible that classical Th22 cells are "programmed" to differentiate into Th17 cells, as has been shown for cells precommitted to Th1 differentiation (34). The commitment and flexibility of effector T cell populations are probably controlled by the expression and balance of lineage-specifying transcription factors (35). In support of that assumption, our results showed that the nonclassical, but not the classical, Th22 cells in blood and peritumoral liver and tumor tissues from HCC patients expressed T-bet and/or RORγt at a level comparable to that exhibited by Th1 and/or Th17 cells. It is plausible that under certain conditions of local stimulation, Th22 cells in tissues can differentiate into polyfunctional T cells that trigger additional responses. Thus, whereas IL-22 and IL-17 may induce cancer growth and angiogenesis, it is possible that IFN-γ suppresses the proliferation and survival of tumor cells.

An unexpected finding is that Th22 expansion and polarization were efficiently elicited by activated monocytes and, to a lesser extent, also by monocyte-derived Mφ or DCs. This difference in T cell–polarizing capacity correlates with the pattern of cytokines produced by the various stimulated APCs. Indeed, when activated by LPS and Pam3CysSK4, monocytes produced larger amounts of TNF-α, IL-1β, IL-23, IL-6, and TGF-β. One of those molecules, IL-1β, proved to play a dominant role in the induction of IFN-γ–related Th22 subsets, whereas TGF-β mainly stimulated the IL-17–expressing Th22 subsets. These findings agree with the widespread views that IL-1β efficiently activates Th1 responses, whereas TGF-β is involved in Th17 cell development (18, 36, 37). Our results also suggest that nonclassical Th22 subsets are expanded from memory $CD4^+$ T cells, which concurred with our earlier study showing that activated monocytes from HCC tissue can intensively expand Th17/Th1 cells only from the memory effector T cells (18). The Th22 cells expanded from naive T cells were not well marked but exhibited a classical phenotype, thus revealing that extra induction processes are required for such cell development. Further research is needed to identify the APCs and maturation stimuli other than microbial products that can induce Th22 responses in vivo under other physiological and pathological conditions.

B7-H1 is a cell-surface glycoprotein that belongs to the B7 family of cosignaling molecules and has a profound regulatory effect on T cell responses (38–40). The present study reveals what we believe to be a novel role of B7-H1 in regulating Th22 subset polarization in human tumors, and this conclusion is supported by the results of 3 sets of experiments. First, although both peritumoral liver and paired tumor monocytes had a marked impact on cytokine production, only monocytes isolated from tumor tissue showed pronounced B7-H1 expression, and most Th22 cells isolated from corresponding tissue did not produce IFN-γ. Second, the monocytes isolated from peritumoral liver tissue were more potent in promoting the expansion of IFN-γ–producing Th22 cells, whereas paired tumor monocytes were selectively linked to the IL-17–expressing Th22 subsets; blocking B7-H1 by preincubating tumor monocytes with the mAb MIH1 directed Th22 differentiation toward IFN-γ. Third, expression of the B7-H1 receptor PD-1 was significantly increased on tumor-infiltrating Th cells; briefly, in HCC tissue, a striking inverse association was found between the levels of $PD\text{-}1^+$ Th cells and IFN-γ–producing, but not Th17-expressing, Th22 cells. Therefore, if $B7\text{-}H1^+$–activated monocytes can defeat the formation of IFN-γ–related Th22 subsets, it may reflect a novel immunoediting mechanism in human tumors.

Recent clinical trials with anti–B7-H1/PD-1 mAbs have demonstrated clinical activity in patients with advanced solid tumors (41, 42). Interestingly, B7-H1 expression in tumor specimens was found to be associated with the objective response in patients treated with anti–PD-1 mAbs (43). It should be noted that the upregulation of B7-H1 in tumor tissues can also be viewed as a reflection of endogenous inflammatory immune responses, but not simply as the dominance of immune suppression (44). In a pre-

vious study, we observed that the activated monocytes in HCC tissue express B7-H1 to suppress tumor-specific T cell function (38, 39). The present study showed that B7-H1–expressing monocytes could skew Th22 polarization away from IFN-γ and toward IL-17, which may promote tumor progression by fostering angiogenesis. Thus, in addition to reversing immune tolerance, blockade of the B7-H1/PD-1 axis may also regulate tumor angiogenesis. A better understanding of the mechanisms of B7-H1/PD-1 interaction in tumor environments would be helpful for developing rational treatment combinations with mAbs blocking PD-1 or B7-H1 and other potentially synergistic therapeutic agents, including those targeting angiogenesis.

Methods

Patients and specimens. Liver and tumor tissue samples were obtained from HCC patients during surgery at the Cancer Center of Sun Yat-sen University (Supplemental Tables 1 and 2). None of the patients had received anticancer therapy before the sampling, and individuals with concurrent autoimmune disease, HIV, or syphilis were excluded. Paired samples of blood, peritumoral liver tissue (taken 0.5–2 cm distal to the tumor site), and tumor tissue from 32 HCC patients who received treatment between 2010 and 2014 (cohort 1; Supplemental Tables 1 and 2) were used to isolate peripheral and tissue-infiltrating leukocytes. An additional 197 HCC patients who had undergone curative resection between 2002 and 2007 and had complete follow-up data (cohort 2; Supplemental Table 2) were enrolled for analysis of OS and DFS. Samples of normal liver were obtained distal to liver hemangiomas (Supplemental Table 1). Clinical stages were classified according to the guidelines of the International Union against Cancer. All samples were anonymously coded in accordance with local ethical guidelines (as stipulated by the Declaration of Helsinki).

Isolation of mononuclear cells from peripheral blood and tissues. Peripheral leukocytes were isolated by Ficoll density gradient centrifugation (45). Fresh tissue–infiltrating leukocytes were obtained as described elsewhere (46). In short, liver biopsy specimens were cut into small pieces and digested in RPMI 1640 (HyClone Laboratories) supplemented with 0.05% collagenase IV (Sigma-Aldrich), 0.002% DNase I (Roche), and 20% FBS (HyClone Laboratories) at 37°C for 1 hour. Dissociated cells were filtered through a 150-mm mesh and separated by Ficoll centrifugation, and the mononuclear cells were washed and resuspended in RPMI 1640 supplemented with 10% FBS. In some experiments, tissue-infiltrating monocytes were purified from the mononuclear cells using anti-CD14 magnetic beads (Miltenyi Biotec) according to the manufacturer's instructions. Of note, over 95% of tissue-derived $CD14^+$ cells exhibited a $CD14^{hi}$ phenotype and did not express the resident monocyte marker CD16 or DC markers CD1a and CD83 (data not shown).

Flow cytometry. Monocytes, Mφ, and DCs from peripheral blood, tissues, or in vitro culture were stained with fluorochrome-conjugated Abs and then analyzed by flow cytometry (46). The peripheral lymphocytes, tissue-infiltrating lymphocytes, and T cells from in vitro culture were stimulated at 37°C for 5 hours with Leukocyte Activation Cocktail (BD Pharmingen). Thereafter, cells were stained with surface markers, fixed and permeabilized with IntraPrep reagent (Beckman Coulter), and finally stained with intracellular markers. Data were acquired on a Gallios Flow Cytometer (Beckman Coulter). The fluorochrome-conjugated Abs used are described in Supplemental Table 4.

In vitro culture system for monocytes, Mφ, and DCs. Monocytes were purified from normal peripheral blood mononuclear cells (PBMCs) using anti-CD14 magnetic beads (Miltenyi Biotec) according to the manufacturer's instructions. The purified $CD14^+$ cells were cultured for 18 hours in DMEM containing 10% human AB serum in the presence or absence of Pam3CysSK4 (1 μg/ml; Invivogen), LPS (100 ng/ml; Sigma-Aldrich), poly (I:C) (5 μg/ml; Sigma-Aldrich), or CpG ODN (5 μg/ml; Invivogen). In some experiments, Mφ and DCs were generated from purified monocytes as described elsewhere (19, 20). In short, to generate DCs, the purified monocytes were cultured for 6 days in complete RPMI medium supplemented with granulocyte-macrophage-CSF (GM-CSF) (40 ng/ml) and IL-4 (40 ng/ml) (R&D Systems), and half of the culture medium was replaced on days 3 and 5. In parallel, the monocytes in RPMI medium containing 10% human AB serum were cultured for 6 days to obtain Mφ. Thereafter, these monocyte-derived cells were left untreated or were stimulated with Pam3CysSK4 (1 μg/ml), LPS (100 ng/ml), poly (I:C) (5 μg/ml), or CpG ODN (5 μg/ml) for 18 hours.

ELISA. Concentrations of TNF-α, IL-1β, IL-6, IL-12p70, IL-23, and TGF-β in the culture supernatants of monocytes, Mφ, and DCs were detected using ELISA kits according to the manufacturers' instructions (kits for TNF-α, IL-1β, IL-6, IL-12p70, and IL-23 were from eBioscience; the kit for TGF-β was from BD Pharmingen).

Construction of B7-H1 and B7-DC expression plasmids and stable transfection. B7-H1 and B7-DC were cloned into EcoRI and BamHI sites of the retroviral vector pBABE-puro. The retroviral vector pBABE-puro was cotransfected with the helper plasmids pCL-ampho into HEK293T cells using Lipofectamine 2000 (Invitrogen) according to the manufacturer's instructions. Culture supernatants containing recombinant viral particles were harvested and used to infect HEK293T cells in the presence of polybrene (2.5 μg/ml; Sigma-Aldrich). To establish stable cell lines, HEK293T cells were selected with puromycin (4 μg/ml; Calbiochem) on day 3 after infection.

In vitro T cell culture system. In 2-day incubations, purified autologous T cells, naive T cells, and memory T cells (Miltenyi Biotec) were left untreated, cultured with various APCs or tissue-derived monocytes (5:1), or exposed to medium supplemented with recombinant IL-1β (2 ng/ml), IL-6 (10 ng/ml), IL-23 (1 ng/ml), and/or TGF-β (5 ng/ml) (all cytokines from R&D Systems) in the presence of 2 μg/ml anti-CD3 and 2 μg/ml anti-CD28 (eBioscience). Thereafter, the cells were washed and maintained in RPMI medium supplemented with 20 IU/ml IL-2 (eBioscience) for the indicated times (Figure 3, B–H and Figure 4, C–F.) in the presence of different cells or cytokines. In some cases, autologous T cells were pretreated with a neutralizing Ab against TNF-α (1 μg/ml), IL-1β (10 μg/ml), IL-6 (25 μg/ml), IL-23 (10 μg/ml), or TGF-β (10 μg/ml) (all from R&D Systems), a blocking Ab against B7-H1 (eBioscience), or a control IgG (R&D Systems) and were then exposed to the indicated cells (5:1) (Figure 3E and Figure 4, C and D); in other cases, T cells were pretreated with a specific inhibitor for STAT1 (fludarabine, 50 μM) or STAT3 (AG490, 50 μM) (both from Sigma-Aldrich) or were incubated with 10 μg/ml mitomycin C–pretreated mock-293T, B7-H1-293T, or B7-DC-293T cells in the presence or absence of a blocking Ab against B7-H1 or control IgG and subsequently exposed to conditioned media from LPS-activated monocytes or the indicated cytokines (Figure 4, E and F). Notably, the neutralizing antibodies (against B7-H1 or against cytokines) were present throughout the entire culture processes.

Real-time PCR. Total RNA of peripheral, peritumoral, and tumor monocytes from HCC patients was isolated using TRIzol reagent (Invitrogen). Aliquots containing 2 μg total RNA were reverse transcribed using Moloney murine leukemia virus (M-MLV) reverse transcriptase (Promega). The specific primers used to amplify the genes are listed in Supplemental Table 5. PCR was performed in triplicate using SYBR Green Real-time PCR MasterMix (TOYOBO) in a Roche LightCycler 480 System. All results are presented in arbitrary units relative to 18S rRNA expression.

Immunohistochemistry and immunofluorescence. Paraffin-embedded and formalin-fixed HCC samples were cut into 5-μm sections, which were then processed for immunohistochemistry as previously described (47). Following incubation with an Ab against human IL-22 or CD34 (both from Abcam), the sections were stained in an EnVision System (Dako). For immunofluorescence analysis, tissues were stained with rabbit anti-human CD3, mouse anti-human PD-1, and goat anti-human IL-22, followed by Alexa Fluor 488–conjugated anti-mouse IgG, Alexa Fluor 555–conjugated anti-rabbit IgG, and Alexa Fluor 633–conjugated anti-goat IgG (Molecular Probes). Positive cells were quantified using Image-Pro Plus software (MediaCybernetics) and detected by confocal microscopy.

Evaluation of immunohistochemical variables. Analysis was performed by 2 independent observers who were blinded to the clinical outcome (48). The tissue sections were screened in an inverted research microscope (model DM IRB; Leica) at low magnification (×100), and the 5 most representative fields were selected. Thereafter, the respective areas were measured at ×400 magnification, and the nucleated IL-22$^+$ cells in each area were counted and expressed as the number of cells per field.

Immunoblotting. The proteins were extracted as previously described (19). Equal amounts of cellular proteins were separated by 10% SDS-PAGE, immunoblotted with the indicated Abs (Supplemental Table 6), and visualized using an ECL kit.

In vivo tumor assay. Hepatoma cells (HepG2, 10^6 cells) in 100 μl of buffered saline were subcutaneously injected into the dorsal tissue of 5- to 6-week-old male NOD/SCID mice. T cells (2.5×10^6) polarized by tumor monocytes in the presence or absence of anti–B7-H1 mAb (eBioscience) in 100 μl of buffered saline were subsequently injected into the peritoneum of the male mice on day 3 after the HepG2 inoculation. Thereafter, the animals were injected with Abs against human IL-22 and IL-17 (10 mg/kg) in 100 μl buffered saline into the peritoneum every 3 days. In parallel, control animals were injected with buffered saline. Tumor volume was calculated based on 3 perpendicular measurements.

In another set of in vivo experiments, 10^6 hepatoma cells (HepG2) in 100 μl buffered saline were subcutaneously injected into the dorsal tissue of male NOD/SCID mice. Thereafter, the animals were injected with IL-22 (50 ng) alone, or IL-22 (50 ng) plus IL-17 (50 ng) or plus IFN-γ (50 ng) in 100 μl buffered saline into the dorsal tissue every 3 days. In parallel, control animals were injected with buffered saline. Tumor volume was calculated based on 3 perpendicular measurements. After 15 days, the tumors were excised, fixed, embedded in paraffin, and sectioned, after which the paraffin-embedded sections were immunostained with an Ab against mouse CD34 (BioLegend).

Statistics. Results are expressed as means ± SEM. The statistical significance of differences between groups was determined using a Student's *t* test. Cumulative survival time was calculated by the Kaplan-Meier method, and survival was measured in months from resection to recurrence or from the last review. The log-rank test was applied to compare the groups. Multivariate analyses of prognostic factors for OS and DFS were performed using the Cox proportional hazards model. SPSS statistical software, version 13.0 (SPSS Inc.) was used for all statistical analyses. All data were analyzed using 2-tailed tests unless otherwise specified, and a P value of less than 0.05 was considered statistically significant.

Study approval. For experiments using human samples, written informed consent was obtained from the patients, and the protocol was approved by the IRB of Sun Yat-sen University (Guangzhou, China). All animal experiments were performed with the approval of the IACUC of Sun Yat-sen University (Guangzhou, China).

Acknowledgments

We thank Patricia Ödman for editing the manuscript. The study was supported by project grants from the National Natural Science Foundation of China (81422036, 81171982, and 81230073); the Ministry of Health of China (2012ZX10002-011); the Guangdong Natural Science Funds for Distinguished Young Scholar (S2013050014639); the Program for New Century Excellent Talents in University of the Ministry of Education of China (NCET-11-0534); and the Foundation for the Author of National Excellent Doctoral Dissertation of PR China (201230).

Address correspondence to: Limin Zheng or Dong-Ming Kuang, School of Life Sciences, Sun Yat-sen University, 135 Xin Gang Xi Lu, Guangzhou 510275, China. Phone: 86.20.84112163; E-mail: zhenglm@mail.sysu.edu.cn (L. Zheng). Phone: 86.20.84112157; E-mail: kdming@mail.sysu.edu.cn (D.M. Kuang).

1. Wolk K, Sabat R. Interleukin-22: a novel T- and NK-cell derived cytokine that regulates the biology of tissue cells. *Cytokine Growth Factor Rev*. 2006;17(5):367–380.
2. Sonnenberg GF, Fouser LA, Artis D. Border patrol: regulation of immunity, inflammation and tissue homeostasis at barrier surfaces by IL-22. *Nat Immunol*. 2011;12(5):383–390.
3. Rubino SJ, Geddes K, Girardin SE. Innate IL-17 and IL-22 responses to enteric bacterial pathogens. *Trends Immunol*. 2012;33(3):112–118.
4. Kamanaka M, et al. Memory/effector (CD45RB(lo)) CD4 T cells are controlled directly by IL-10 and cause IL-22-dependent intestinal pathology. *J Exp Med*. 2011;208(5):1027–1040.
5. Qin WZ, et al. Expressions of IL-22 in circulating CD4+/CD8+ T cells and their correlation with disease activity in SLE patients. *Clin Exp Med*. 2011;11(4):245–250.
6. Feng D, et al. Interleukin-22 promotes proliferation of liver stem/progenitor cells in mice and patients with chronic hepatitis B virus infection. *Gastroenterology*. 2012;143(1):188–198.
7. Mitra A, Raychaudhuri SK, Raychaudhuri SP. Functional role of IL-22 in psoriatic arthritis. *Arthritis Res Ther*. 2012;14(2):R65.
8. Ma HL, et al. IL-22 is required for Th17 cell-mediated pathology in a mouse model of psoriasis-like skin inflammation. *J Clin Invest*. 2008;118(2):597–607.
9. Eyerich S, et al. Th22 cells represent a distinct human T cell subset involved in epidermal immunity and remodeling. *J Clin Invest*. 2009;119(12):3573–3585.
10. Gurney AL. IL-22, a Th1 cytokine that targets the pancreas and select other peripheral tissues. *Int Immunopharmacol*. 2004;4(5):669–677.
11. Zheng Y, et al. Interleukin-22, a TH17 cytokine, mediates IL-23-induced dermal inflammation and

acanthosis. *Nature*. 2007;445(7128):648–651.
12. Ma HL, et al. IL-22 is required for Th17 cell-mediated pathology in a mouse model of psoriasis-like skin inflammation. *J Clin Invest*. 2008;118(2):597–607.
13. Liang SC, et al. Interleukin (IL)-22 and IL-17 are coexpressed by Th17 cells and cooperatively enhance expression of antimicrobial peptides. *J Exp Med*. 2006;203(10):2271–2279.
14. Duhen T, Geiger R, Jarrossay D, Lanzavecchia A, Sallusto F. Production of interleukin 22 but not interleukin 17 by a subset of human skin-homing memory T cells. *Nat Immunol*. 2009;10(8):857–863.
15. Trifari S, Kaplan CD, Tran EH, Crellin NK, Spits H. Identification of a human helper T cell population that has abundant production of interleukin 22 and is distinct from T(H)-17, T(H)1, and T(H)2 cells. *Nat Immunol*. 2009;10(8):864871.
16. Reis e Sousa C. Activation of dendritic cells: translating innate into adaptive immunity. *Curr Opin Immunol*. 2004;16(1):21–25.
17. Zhou J, Ding T, Pan W, Zhu LY, Li L, Zheng L. Increased intratumoral regulatory T cells are related to intratumoral macrophages and poor prognosis in hepatocellular carcinoma patients. *Int J Cancer*. 2009;125(7):1640–1648.
18. Kuang DM, Peng C, Zhao Q, Wu Y, Chen MS, Zheng L. Activated monocytes in peritumoral stroma of hepatocellular carcinoma promote expansion of memory T helper 17 cells. *Hepatology*. 2010;51(1):154–164.
19. Kuang DM, Wu Y, Chen N, Cheng J, Zhuang SM, Zheng L. Tumor-derived hyaluronan induces formation of immunosuppressive macrophages through transient early activation of monocytes. *Blood*. 2007;110(2):587–595.
20. Kuang DM, Zhao Q, Xu J, Yun JP, Wu C, Zheng L. Tumor-educated tolerogenic dendritic cells induce CD3epsilon down-regulation and apoptosis of T cells through oxygen-dependent pathways. *J Immunol*. 2008;181(5):3089–3098.
21. Liu T, et al. Increased circulating Th22 and Th17 cells are associated with tumor progression and patient survival in human gastric cancer. *J Clin Immunol*. 2012;32(6):1332–1339.
22. Kirchberger S, et al. Innate lymphoid cells sustain colon cancer through production of interleukin-22 in a mouse model. *J Exp Med*. 2013;210(5):917–931.
23. Kim K, Kim G, Kim JY, Yun HJ, Lim SC, Choi HS. Interleukin-22 promotes epithelial cell transformation and breast tumorigenesis via MAP3K8 activation. *Carcinogenesis*. 2014;35(6):1352–1361.
24. Kryczek I, et al. IL-22(+)CD4(+) T cells promote colorectal cancer stemness via STAT3 transcription factor activation and induction of the methyltransferase DOT1L. *Immunity*. 2014;40(5):772–784.
25. Xu X, et al. Increased intratumoral interleukin 22 levels and frequencies of interleukin 22-producing $CD4^+$ T cells correlate with pancreatic cancer progression. *Pancreas*. 2014;43(3):470–477.
26. Jiang R, et al. Interleukin-22 promotes human hepatocellular carcinoma by activation of STAT3. *Hepatology*. 2011;54(3):900–909.
27. Kong X, et al. Interleukin-22 induces hepatic stellate cell senescence and restricts liver fibrosis. *Hepatology*. 2012;56(3):1150–1159.
28. Wolk K, et al. IL-22 regulates the expression of genes responsible for antimicrobial defense, cellular differentiation, and mobility in keratinocytes: a potential role in psoriasis. *Eur J Immunol*. 2006;36(5):1309–1323.
29. Lee YK, et al. Late developmental plasticity in the T helper 17 lineage. *Immunity*. 2009;30(1):92–107.
30. Siegmund K, et al. Unique phenotype of human tonsillar and in vitro-induced $FOXP3^+$ $CD8^+$ T cells. *J Immunol*. 2009;182(4):2124–2130.
31. Kryczek I, et al. $IL\text{-}17^+$ regulatory T cells in the microenvironments of chronic inflammation and cancer. *J Immunol*. 2011;186(7):4388–4395.
32. Annunziato F, et al. Phenotypic and functional features of human Th17 cells. *J Exp Med*. 2007;204(8):1849–1861.
33. Messi M, Giacchetto I, Nagata K, Lanzavecchia A, Natoli G, Sallusto F. Memory and flexibility of cytokine gene expression as separable properties of human TH1 and TH2 lymphocytes. *Nat Immunol*. 2003;4(1):78–86.
34. Rivino L, Messi M, Jarrossay D, Lanzavecchia A, Sallusto F, Geginat J. Chemokine receptor expression identifies Pre-T helper (Th)1, Pre-Th2, and nonpolarized cells among human $CD4^+$ central memory T cells. *J Exp Med*. 2004;200(6):725–735.
35. Zhou L, et al. TGF-β-induced Foxp3 inhibits TH17 cell differentiation by antagonizing RORgammat function. *Nature*. 2008;453(7192):236–240.
36. McGeachy MJ, et al. TGF-β and IL-6 drive the production of IL-17 and IL-10 by T cells and restrain T(H)-17 cell-mediated pathology. *Nat Immunol*. 2007;8(12):1390–1397.
37. Volpe E, et al. A critical function for transforming growth factor-beta, interleukin 23 and proinflammatory cytokines in driving and modulating human T(H)-17 responses. *Nat Immunol*. 2008;9(6):650–657.
38. Zhao Q, et al. Interleukin-17-educated monocytes suppress cytotoxic T-cell function through B7-H1 in hepatocellular carcinoma patients. *Eur J Immunol*. 2011;41(8):2314–2322.
39. Kuang DM, et al. Activated monocytes in peritumoral stroma of hepatocellular carcinoma foster immune privilege and disease progression through PD-L1. *J Exp Med*. 2009;206(6):1327–1337.
40. Zou W, Chen L. Inhibitory B7-family molecules in the tumour microenvironment. *Nat Rev Immunol*. 2008;8(6):467–477.
41. Brahmer JR, et al. Safety and activity of anti-PD-L1 antibody in patients with advanced cancer. *N Engl J Med*. 2012;366(26):2455–2465.
42. McDermott DF, Atkins MB. PD-1 as a potential target in cancer therapy. *Cancer Med*. 2013;2(5):662–673.
43. Topalian SL, et al. Safety, activity, and immune correlates of anti-PD-1 antibody in cancer. *N Engl J Med*. 2012;366(26):2443–2454.
44. Taube JM, et al. Colocalization of inflammatory response with B7-h1 expression in human melanocytic lesions supports an adaptive resistance mechanism of immune escape. *Sci Transl Med*. 2012;4(127):127ra37.
45. Zhao Q, et al. Activated $CD69^+$ T cells foster immune privilege by regulating IDO expression in tumor-associated macrophages. *J Immunol*. 2012;188(3):1117–1124.
46. Kuang DM, et al. Tumor-activated monocytes promote expansion of IL-17-producing $CD8^+$ T cells in hepatocellular carcinoma patients. *J Immunol*. 2010;185(3):1544–1549.
47. Wu Y, Zhao Q, Peng C, Sun L, Li XF, Kuang DM. Neutrophils promote motility of cancer cells via a hyaluronan-mediated TLR4/PI3K activation loop. *J Pathol*. 2011;225(3):438–447.
48. Kuang DM, et al. Peritumoral neutrophils link inflammatory response to disease progression by fostering angiogenesis in hepatocellular carcinoma. *J Hepatol*. 2011;54(5):948–955.